BJR, 2025, **98**, 965–973
https://doi.org/10.1093/bjr/tqaf062
Advance access publication: 19 March 2025
Research Article

Standardized pancreatic MRI-T1 measurement methods: comparison between manual measurement and a semi-automated pipeline with automatic quality control

Alexandre Triay Bagur, PhD*[,1,2], Zobair Arya, PhD[1], Tom Waddell, PhD[1,2], Michele Pansini, MD[3,4], Carolina Fernandes, PhD[1], Daniel Counter[1], Edward Jackson, PhD[1], Helena B. Thomaides-Brears, PhD[1], Matthew D. Robson, PhD[1] Daniel P. Bulte, PhD[2], Rajarshi Banerjee, PhD[1], Paul Aljabar, PhD[1], Michael Brady, PhD[1]

[1]Perspectum Ltd, Oxford OX4 2LL, United Kingdom
[2]Department of Engineering Science, University of Oxford, Oxford OX1 3PJ, United Kingdom
[3]Clinica Di Radiologia EOC, Istituto Di Imaging Della Svizzera Italiana (IIMSI), Ente Ospedaliero Cantonale, Lugano 6900, Switzerland
[4]Department of Radiology, John Radcliffe Hospital, Oxford University Hospitals NHS Foundation Trust, Oxford OX3 0AG, United Kingdom
*Corresponding author: Alexandre Triay Bagur, PhD, Perspectum Ltd, Oxford OX4 2LL, United Kingdom (alexandre.bagur@perspectum.com)

Abstract

Objectives: Scanner-referenced T1 (srT1) is a method for measuring pancreas T1 relaxation time. The purpose of this multi-centre study is 2-fold: (1) to evaluate the repeatability of manual ROI-based analysis of srT1, (2) to validate a semi-automated measurement method with an automatic quality control (QC) module to identify likely discrepancies between automated and manual measurements.

Methods: Pancreatic MRI scans from a scan-rescan cohort (46 subjects) were used to evaluate the repeatability of manual analysis. Seven hundred and eight scans from a longitudinal multi-centre study of 466 subjects were divided into training, internal validation (IV), and external validation (EV) cohorts. A semi-automated method for measuring srT1 using machine learning is proposed and compared against manual analysis on the validation cohorts with and without automated QC.

Results: Inter-operator agreement between manual ROI-based method and semi-automated method had low bias (3.8 ms or 0.5%) and limits of agreement [−36.6, 44.1] ms. There was good agreement between the 2 methods without automated QC (IV: 3.2 [−47.1, 53.5] ms, EV: −0.5 [−35.2, 34.2] ms). After QC, agreement on the IV set improved, was unchanged in the EV set, and the agreement in both was within inter-operator bounds (IV: −0.04 [−33.4, 33.3] ms, EV: −1.9 [−37.6, 33.7] ms). The semi-automated method improved scan-rescan agreement versus manual analysis (manual: 8.2 [−49.7, 66] ms, automated: 6.7 [−46.7, 60.1] ms).

Conclusions: The semi-automated method for characterization of standardized pancreatic T1 using MRI has the potential to decrease analysis time while maintaining accuracy and improving scan-rescan agreement.

Advances in knowledge: We provide intra-operator, inter-operator, and scan-rescan agreement values for manual measurement of srT1, a standardized biomarker for measuring pancreas fibro-inflammation. Applying a semi-automated measurement method improves scan-rescan agreement and agrees well with manual measurements, while reducing human effort. Adding automated QC can improve agreement between manual and automated measurements.

Summary statement: We describe a method for semi-automated, standardized measurement of pancreatic T1 (srT1), which includes automated quality control. Measurements show good agreement with manual ROI-based analysis, with comparable consistency to inter-operator performance.

Keywords: pancreas; T1 mapping; standardised; fibro-inflammation; quality control.

Introduction

There is a continuing surge in the incidence of diseases affecting the pancreas, including pancreatic cancer, chronic pancreatitis, and diabetes.[1] This may reflect the increasing prevalence of metabolic syndrome and obesity, since obesity leads to fat infiltration, which can trigger an inflammatory response and eventually chronic pancreatitis and pancreatic cancer.[2] Fat infiltration in the pancreas has also been linked to rapidly escalating levels of type 2 diabetes[3,4] and metabolic-associated steatotic liver disease (MASLD).[5,6] This motivates the need for methods to assess the pancreas both in disease and incidentally before disease becomes symptomatic.

Quantitative MRI enables non-invasive assessment of the pancreas. For example, one MRI-derived biomarker, T1 relaxation time,[7,8] is sensitive to fibrosis and inflammation and correlates with pancreatic fibrosis.[9] T1 can be used to grade chronic pancreatitis severity and has the potential to aid in its early diagnosis.[10-12] However, its clinical applicability is limited by dependence on field strength, and its poor reproducibility across sites, MRI vendors, and patient populations.[13-15] To counter this, strategies for pancreatic T1 harmonization have used a combination of careful acquisition design, quality assurance, and calibration techniques.[14,16] One such strategy,

Received: 11 April 2024; **Revised:** 20 August 2024; **Accepted:** 12 March 2025

scanner-referenced T1 (srT1 or SR-T1), has been FDA cleared for pancreatic MRI analysis.[17,18]

Even with a standardized quantitative imaging biomarker, manual delineation of the pancreas parenchyma to obtain an aggregate measurement demands expertise and is time-consuming. The intrinsically complex task is further complicated by the presence of the main pancreatic duct and surrounding visceral adipose tissue. One measurement approach used clinically is to place regions of interest (ROIs) within the pancreas on the scan of interest,[11,19-21] targeting homogenous regions of parenchyma.[10] However, ROI placement requires expertise and suffers from sampling bias, notably in heterogeneous disease presentations.

Recent advances in image analysis, as well as the increasing prevalence of pancreatic disease, encourage the adoption of automated image analysis systems that can be delivered at scale, eg, systems that combine organ segmentation, image fusion, and quality control (QC).[22-24] QC in this work refers to the ability to identify spurious input images, assess the quality of the output of a pipeline, and decide whether an analysis should be performed manually before a report can be generated. These abilities can increase analysis efficiency without compromising on accuracy, which increases confidence and likelihood of clinical adoption.[25]

The aims of this study are 2-fold. First, the same-session scan-rescan repeatability of manual srT1 quantification is evaluated to allow comparison with other methods of measuring pancreatic T1. Second, a semi-automated pipeline for srT1 quantification is developed and applied to a large long COVID dataset including pancreatic MRI scans. The method includes a novel pancreas-specific QC module. We test whether srT1 obtained using the semi-automated method agrees with srT1 obtained by manual ROI placement, notably when QC is applied.

Methods

Study design and participants

This retrospective study used pancreatic MRI scans from a scan-rescan cohort and a cohort from the Long COVID trial COVERSCAN (ClinicalTrials.gov ID NCT04369807). All participants were recruited following expression of interest and gave written informed consent.

Intra-scanner scan-rescan datasets of 46 volunteers (n scans = 92) were obtained at 3 imaging sites with Siemens scanners (Siemens Healthineers, Erlangen, Germany): Perspectum Gemini (MAGNETOM Aera 1.5 T, 20 volunteers), Oxford Centre for Magnetic Resonance (OCMR) (MAGNETOM Prisma 3 T, 18 volunteers), and Chenies Mews Imaging Centre (CMIC) London (MAGNETOM Prisma 3 T, eight volunteers), as detailed in Figure 1. The repeat scans were obtained within the same imaging session, after the subject exited and then re-entered the same scanner.

Datasets available from COVERSCAN were also used. COVERSCAN investigates the impact of SARS-CoV-2 infection on the state of multiple organs, as assessed by quantitative MRI, including the heart, liver, pancreas, spleen, and kidneys.[17,26] Subject characteristics have been reported.[17,26] The study received ethical approval by the South Central—Berkshire B Research Ethics Committee (20/SC/0185) and all research was performed in accordance with relevant guidelines and regulations.

The COVERSCAN datasets comprised baseline scans and 6-month follow-up scans from 466 subjects (n scans = 708). Not all subjects had a follow-up scan available.[17] Scanning had been performed at 3 imaging sites: Perspectum Gemini, Mayo Healthcare London (MAGNETOM Vida 3 T), and CMIC London. The Perspectum and Mayo Healthcare scans were randomly assigned to the training set (n = 432) or the internal validation set (n = 185). To evaluate generalizability to a scanner model unseen during training, the CMIC scans (n = 58) were used as an external validation set (Figure 1).

MRI protocol

All MRI datasets comprised 2 scans: a 2D, breath-hold, Modified Look-Locker Inversion recovery (MOLLI); and a 3D, breath-hold, 2-point Dixon T1-weighted scan covering the entire liver, spleen, pancreas, and kidneys. Table S3 contains acquisition parameters for these scans at 1.5 and 3 T.

Raw T1 maps were calculated from the MOLLI data using Perspectum software.[27,28] These were then standardized to obtain srT1 maps. "Scanner referencing" (sr) includes: (a) a scanner normalization step, which involves referencing to a specific MRI scanner of the same field strength; and (b) a field strength adjustment step to 3 T, when applicable.[29,30] Figure S4 shows the effect of T1 standardization on the COVERSCAN cohort.

Description of manual method

Specially trained image analysts were asked to place an ROI in each of the pancreatic head, body, and tail. Each image analyst had been internally certified for using Perspectum software and had at least 6 months' (with up to 5+ years') experience analysing pancreas MRI images for research. In more detail, for each dataset, the pancreas was first delineated on the srT1 map. Then, up to 3 circular ROIs, each 10 mm diameter, were placed within the delineated region. Finally, the median srT1 value after combining voxel values across the ROIs was reported (see Supplementary Material for more details).

All scans were analysed manually for subsequent comparison with the semi-automated method. For the scan-rescan datasets, measurements of inter-operator agreement and intra-operator agreement were also obtained.

Description of semi-automated pancreas analysis method

The semi-automated method performs the following steps:

1) Pancreas segmentation is estimated on the volumetric scan (water-separated image generated by the MRI scanner) using the segmentation model presented previously,[31] and which was retrained to include 113 additional cases from the training set.
2) The 2D srT1 map is aligned with the 3D segmentation using the DICOM reference coordinate system and the image header information. This enables propagation of the 3D segmentation onto the pancreas in the srT1 map, as illustrated in Figure 2.
3) The resulting 2D pancreas segmentation is refined to exclude pixels with poor T1 numerical fits and non-parenchymal tissues such as pancreatic ducts and visceral fat intrusions (see Supplementary Material).
4) Manual QC: an operator (anonymized author initials, 5 years' experience annotating medical images for

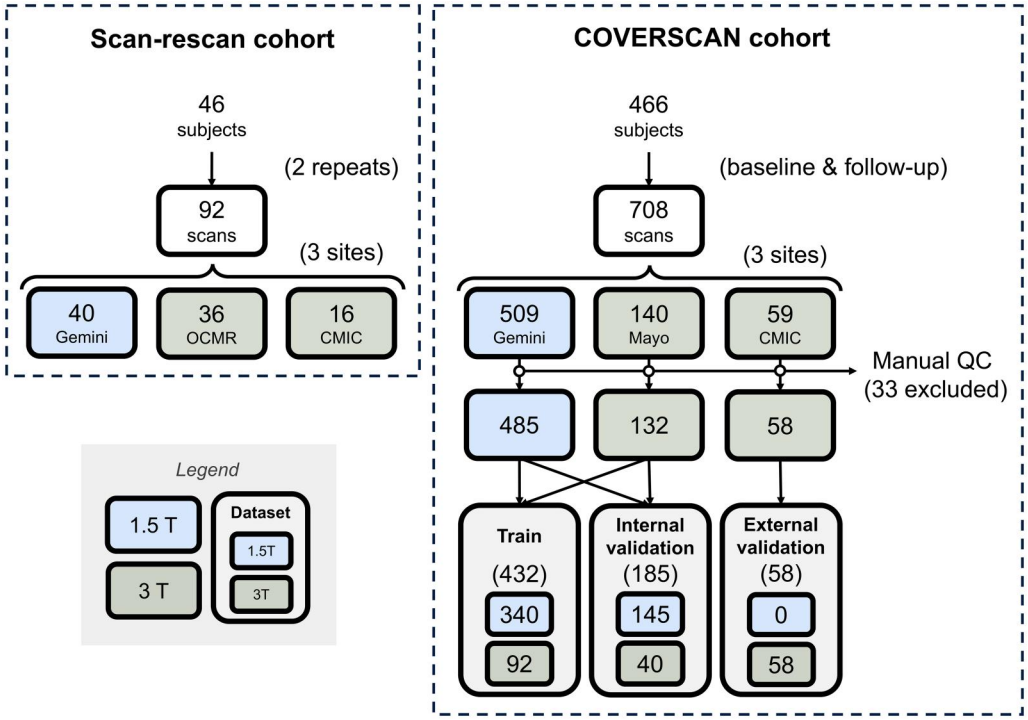

Figure 1. Number of scans and scanner metadata characteristics by study design, for the scan-rescan cohort (left) and the COVERSCAN cohort (right). Manual QC refers to step 4 of the semi-automated method.

research) manually checked the alignment and segmentation. Any failure cases were excluded from further automated analyses. Reasons for exclusion include: segmentations over incorrect structures, incomplete segmentations, misalignments due to subject motion, and artefacts or lesions present within the segmentation.

5) Automated QC: an automated QC module is applied to further flag cases, eg, those that may pass the manual QC in the previous step but may still lead to disagreement between the semi-automated method and manual processing.
6) Reporting of srT1 within the refined segmentation. This srT1 is designed to match the result of manual ROI placement: the 32nd percentile of the srT1 values within the mask is reported (rather than the median value). This percentile was determined on the training set prior to building the automated QC model as the value that led to a non-significant systematic difference between manual and automated measurements. This systematic difference was attributable to ROI sampling effects upon further exploration (see Figure 3, and Supplementary Material for a comparison between manual ROIs, manual delineations and automated segmentations).

Development of automated quality control

The automated QC module was developed by training a linear regression model to predict the amount of discrepancy between srT1 quantification from the manual method and that from the semi-automated method (in ms), where the semi-automatic results were generated *without* the automated QC step. Supplementary Material describes the features and details of building the linear regression model.

Once the QC model was built, a *QC model prediction threshold* was tuned on the training set with the aim of flagging problematic cases during deployment on both validation sets. This threshold was chosen as the value that led to a manual versus auto difference within ±40 ms, ie, within inter-operator agreement; this value was 20 ms.

The semi-automated srT1 values were compared to those from the manual method. To assess the utility of the automated QC module, we also applied the pipeline to the validation sets without automated QC.

Statistical testing

A Wilcoxon signed-rank test was used to assess significance of bias in the Bland-Altman plots. A two-sample *F*-test for equal variances was used to compare the relative change in agreement when using the automated QC module and when not using the automated QC module. The significance level was set to .05.

Results

For the scan-rescan cohort (n scans = 92), the pancreatic srT1 mean ± SD was 719.7 ± 56.6 ms, as quantified by the manual method on the first scan. For the COVERSCAN cohort (n scans = 675), srT1 was 726.8 ± 65.7 ms, as quantified by the manual method.

Technical performance of manual method

Intra-operator, inter-operator, and scan-rescan agreement of the manual method are shown in Table 1. Excellent intra-operator agreement (combined field strengths: bias = −1.7 ms (0.2%), LoA = [−24.6, 21.2] ms, ICC = 0.982), as well as inter-operator agreement (combined field strengths: bias = 3.8 ms (0.5%), LoA = [−36.6, 44.1] ms, ICC = 0.923) were observed. Good repeatability (combined field strengths:

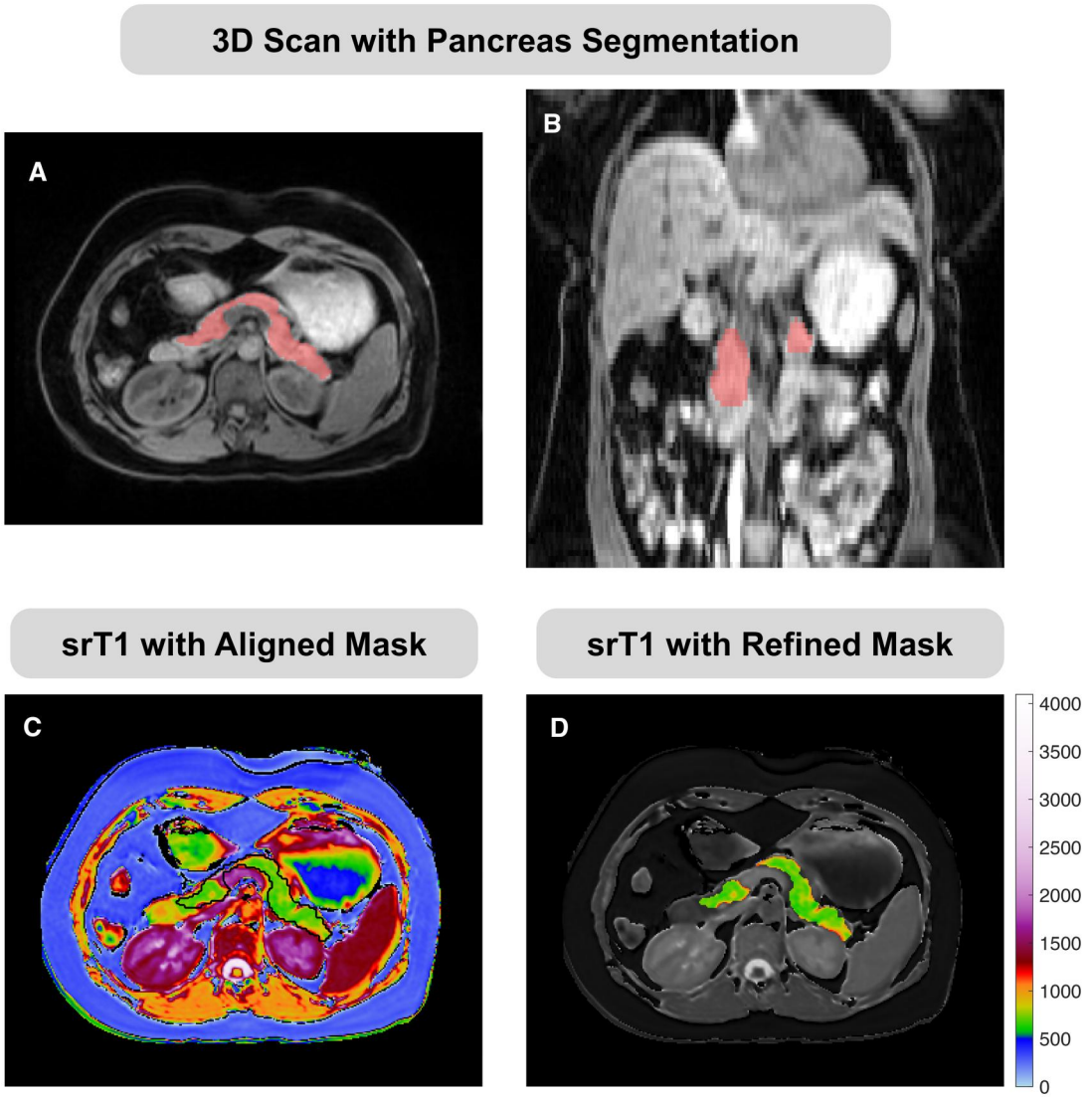

Figure 2. Illustration of the alignment and refinement steps in the semi-automated processing pipeline. The 3D segmentation from the 3D volume (A: axial view, B: coronal view, segmentation as transparent red overlay) is aligned with the 2D srT1 map (C: srT1 map with pancreas mask after alignment, black contour) and then refined (D: srT1 map with pancreas mask after refinement, colour overlay).

bias = 8.2 ms (1.1%), LoA = [−49.7, 66] ms, ICC = 0.846) was observed.

The mean inter-operator agreement (combined field strengths) was used as the target performance bound for the evaluation of the semi-automated method, ie, ±40 ms.

Validation of semi-automated method

Table 1 shows the scan-rescan agreement of the proposed method in the case that neither manual QC nor automated QC were not run, so that the method was fully automated. The results of the automated method (combined field strengths: bias = 6.7 ms (0.9%), LoA = [−46.7, 60.1] ms, ICC = 0.870) were comparable to the manual results.

Figure 4 shows the Bland-Altman agreement between the manual approach and the semi-automated method on the internal validation set and on the external validation set of the COVERSCAN cohort. With no automated QC, the LoA for the internal validation set were [−47.1, 53.5] ms, which is not within the inter-operator agreement LoAs. However, when the QC model was run, the LoA was [−33.4, 33.3] ms with a non-statistically significant bias of −0.04 ms ($P = .7793$). The reduction in LoAs when adding the QC model was statistically significant ($P < .05$). For the external validation set, with no automated QC applied, the LoA was [−35.2, 34.2] ms, which was already within inter-operator LoAs. The agreement when adding automated QC did not improve: with QC, the LoA was [−37.6, 33.7] ms, and the bias of −1.9 ms or 0.2% was not significant ($P = .4494$).

Figure 5 shows srT1 maps from 2 example COVERSCAN scans analysed using the manual method and the proposed semi-automated method, one showing good srT1 agreement (1 ms difference), one showing poor srT1 agreement (55 ms difference).

Discussion

MRI is an important tool in the management of several conditions that affect the pancreas, such as pancreatitis,[32] pancreatic cysts,[33] and pancreatic cancer.[34] Detailed and precise imaging of the pancreas are key to making early and accurate

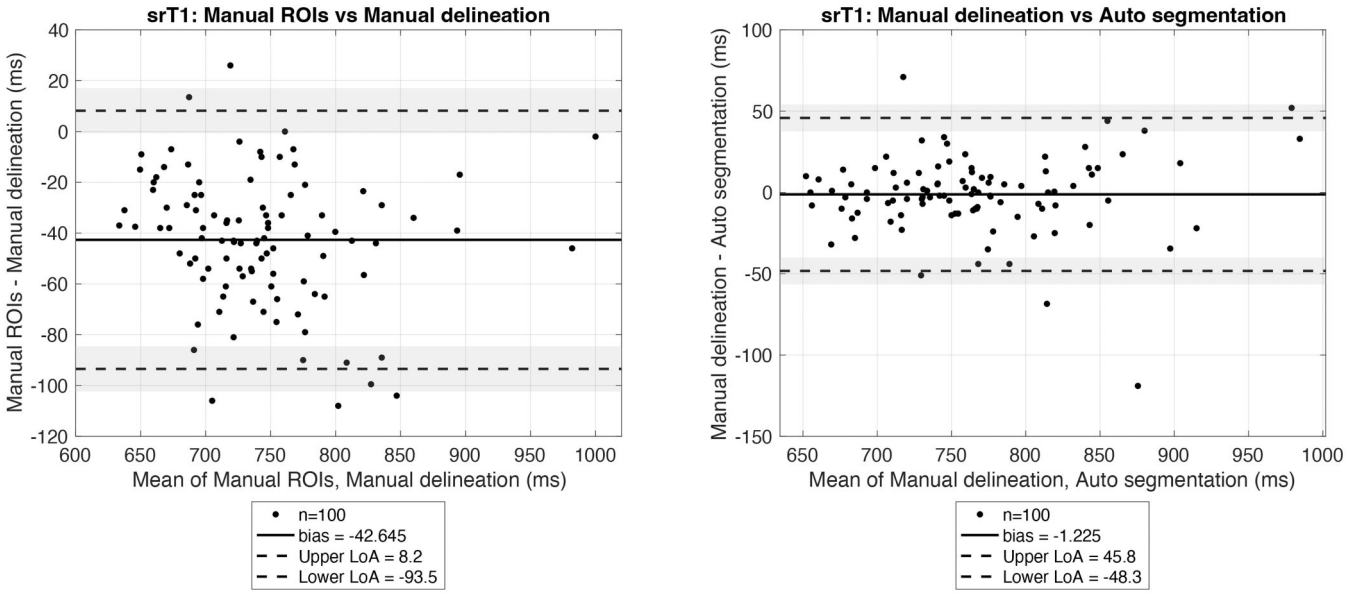

Figure 3. Comparison of srT1 from manual ROIs versus manual delineations (left), and comparison of srT1 from manual delineations versus automated segmentations (right). The srT1 bias between manual ROIs and manual delineations was −42.6 ms in the Bland-Altman analysis and statistically significant ($P < .001$, Wilcoxon signed-rank test), while the srT1 bias between manual delineations and automated delineations was −1.2 ms and not statistically significant ($P = .8364$) (see Supplementary Materials for more details).

Table 1. Results on the same-session scan-rescan cohort.[a]

	1.5T (20 pairs)	3T (26 pairs)	Combined (46 pairs)
Manual			
Intra-operator agreement	−1.7 [−22, 18.6] ms ICC = 0.985, RC = 20.0	−1.7 [−26.7, 23.4] ms ICC = 0.979, RC = 24.8	−1.7 [−24.6, 21.2] ms ICC = 0.982, RC = 22.9
Inter-operator agreement	−3.2 [−38.8, 32.4] ms ICC = 0.856, RC = 35.2	8.8 [−32.6, 50.3] ms ICC = 0.915, RC = 44.2	3.8 [−36.6, 44.1] ms ICC = 0.923, RC = 40.6
Same-session scan-rescan agreement	10.0 [−34.0, 54.0] ms ICC = 0.704, RC = 47.1	6.8 [−60.6, 74.1] ms ICC = 0.841, RC = 67.4	8.2 [−49.7, 66] ms ICC = 0.846, RC = 59.4
Automated			
Same-session scan-rescan agreement	9.1 [−35.2, 53.4] ms ICC = 0.789, RC = 46.8	4.9 [−55.2, 65.0] ms ICC = 0.873, RC = 59.7	6.7 [−46.7, 60.1] ms ICC = 0.870, RC = 54.4

[a]Manual method was also evaluated for intra-operator and inter-operator agreement. Results are shown as bias [lower and upper LoA] of srT1 in ms. LoA: limits of agreement, ICC: intraclass correlation coefficient, RC: repeatability coefficient.

diagnoses. To facilitate these clinical applications, we have introduced a semi-automated method for pancreas MRI quantification with QC.

The method showed excellent agreement with manual ROI-based processing (measured using LoA), with the introduction of the QC module significantly improving agreement between methods. Furthermore, the systematic difference between an ROI-based method and a segmentation-based method was addressed by reporting a percentile of the distribution of voxels within the pancreas segmentation (instead of the median value). We hypothesize that this arises because trained users are instructed to place ROIs in regions that are well within the pancreas parenchyma, and to avoid the pancreatic duct. This leads to ROIs being preferentially placed in homogeneous regions that tend to have lower T1. The reported srT1 scan-rescan repeatability for both methods (within ±40 ms) does not reach clinical significance, as cases with even mild chronic pancreatitis are shown to differ by more than 200 ms (at 3 T).[10,11,35]

The method was applied to quantitative maps of srT1 from the Long COVID study and compared to manual inter-operator performance. Long COVID, an ongoing health concern, can manifest with varied complications, including gastrointestinal issues that necessitate accurate pancreatic evaluation. For example, the COVERSCAN trial found 20% of subjects with pancreatic impairment.[17,26] The validation of the method presented here using data from such a complex and important clinical use case underscores its relevance, robustness, and reliability. The semi-automated pipeline can be seamlessly integrated into the image analysis workflow as decision support and represents a scalable solution for increased robustness and efficiency. Although our method has been applied to srT1, it may apply to analysis of other quantitative maps, provided that metrics are standardized across MRI vendors and field strengths, and the QC module is retrained appropriately.

The semi-automated pipeline offers the potential for more advanced pancreatic measurements, eg, assessment of the head, body, and tail, enabling more precise characterization of disease spread and intensity.[36] For example, in pancreatic cancer, understanding of tumour location and extent could influence surgical planning and prognosis. Similarly, pancreatitis may affect the pancreas segments differently. Beyond the anatomical delineation and traditional whole-organ volume

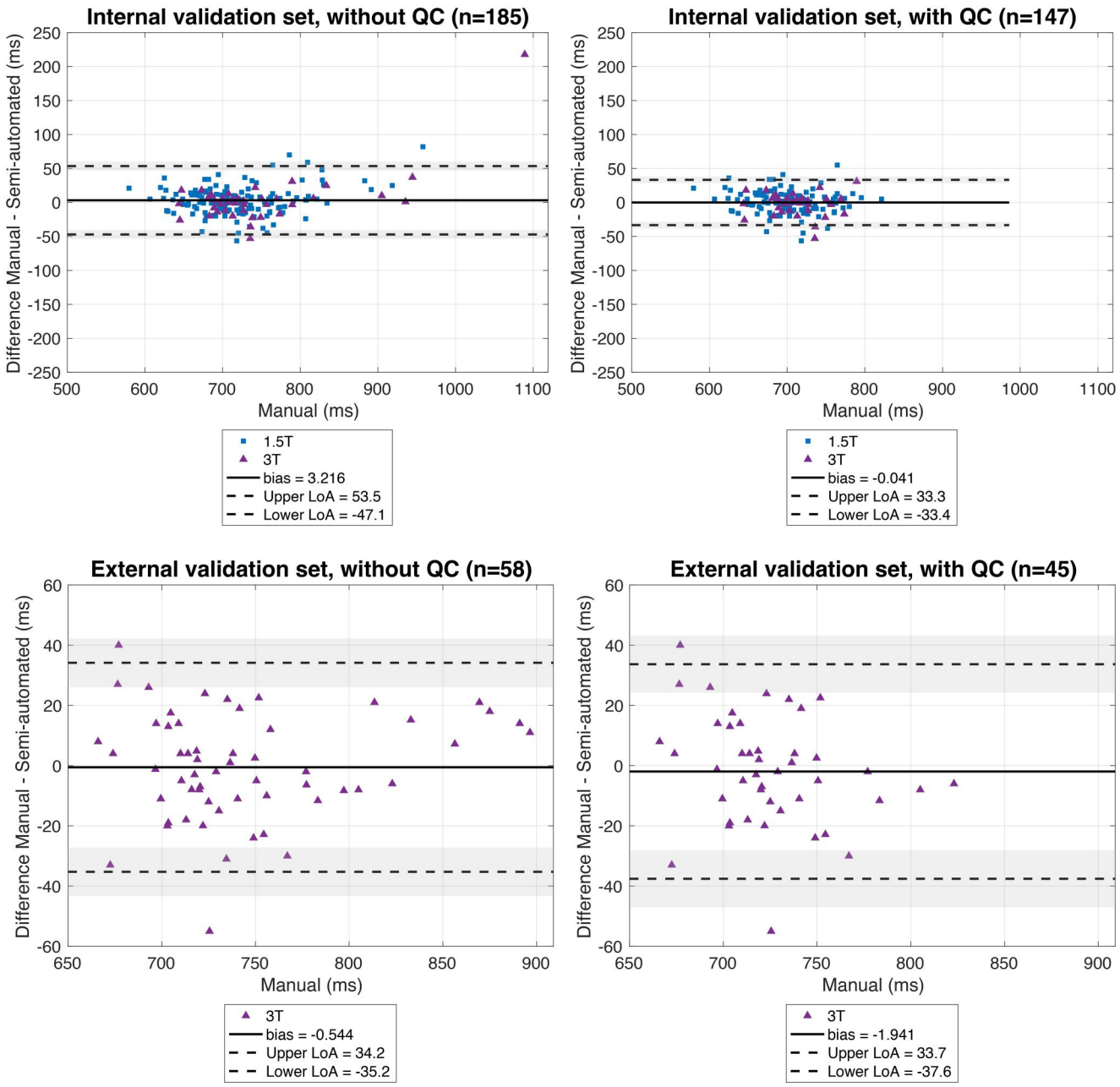

Figure 4. Results on the COVERSCAN validation sets. Bland-Altman agreement of semi-automated method and manual method was evaluated on the internal validation set and on the external validation set, with and without QC. Results are shown as bias [lower and upper LoA] of srT1 in ms. LoA: limits of agreement.

measurements,[37,38] the pipeline holds promise for developing novel biomarkers, such as the volumes of individual pancreatic segments. While the link between these potential new biomarkers and actual disease states and outcomes needs further investigation, the automated pipeline may facilitate such investigations, especially in very large datasets where manual measurements—or manual QC—is infeasible. Furthermore, while the initial application has been in the context of Long COVID, the implications in other clinical scenarios, such as diabetes, or pancreatic disease, warrant dedicated research.

Our results showed that 76% (79% of those 95.3% that passed manual QC) of datasets did not require end-to-end manual analysis, enabling scalable pancreas image analysis. However, the actual increase in efficiency requires a further prospective study. It is crucial that any such system flags cases that need expert manual review, for instance those affected by artefacts or intricate pathology. This increases efficiency, because only prefiltered, more challenging datasets need to be analysed in detail. Based on their experience, knowledge, and training, a manual reader can often deal with images that are challenging for semi-automated processing.

In clinical practice, cases that fail manual QC, especially those with poor segmentation, may be sent back for retraining of the segmentation algorithm, in an active learning framework. Nevertheless, only 33 of 708 (4.7%) datasets were flagged by manual QC in this work. A further advantage of the manual QC is that it enables pre-filtering of the data that may be subsequently used to train and test any

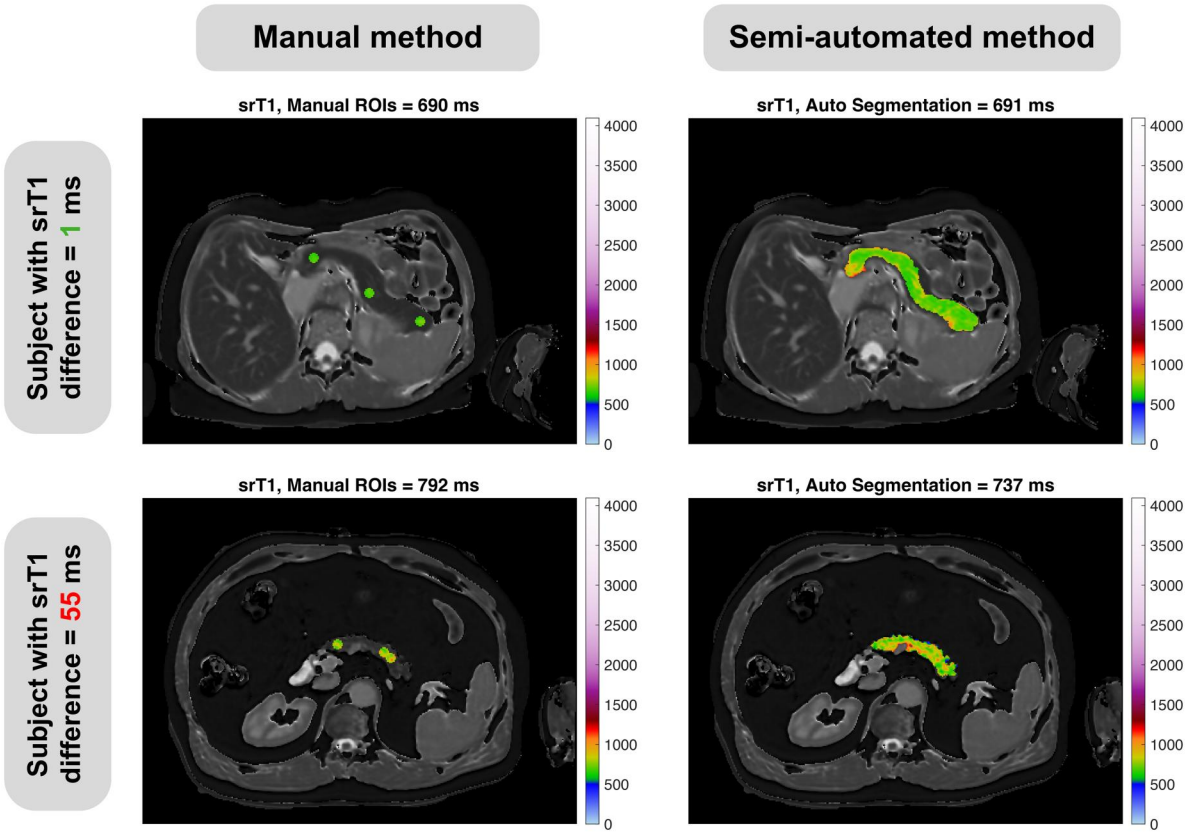

Figure 5. srT1 maps for 2 example scans from the internal validation set after QC was applied. Both good (top) and poor (bottom) agreement between the manual method (circular ROIs) and the semi-automated method (segmentation-based) are represented. ROI: region-of-interest.

regression or machine learning algorithm. This enables more efficient training with a smaller sample size. Conversely, including such images in the training for a pancreas image analysis system would either complicate learning, require a larger dataset, or lower the quality of the prediction model.

In clinical settings, additional automated metrics could further refine the semi-automated method. For example, assessment of the pancreas morphology could provide surrogate information on alterations associated with certain pathologies. Textural features could bring insights into tissue characteristics that are indicative of disease states. Representation learning outputs could help detect anomalous cases, potentially indicating rare or complex conditions that may require additional investigation. This would ensure that the method adapts to the broad spectrum of clinical scenarios encountered in pancreatic MRI.

Limitations

This work had several limitations. First, the MRI datasets in this work were all acquired on Siemens scanners. In future, data from multiple manufacturers will be added to inform the cross-vendor reproducibility of srT1 and of our method. Nevertheless, both clinical field strengths and 3 different scanner models were represented. Additionally, for method development, the scan at baseline and 6-month follow-up were assumed to be independent, given that the changes in srT1 observed over 6 months were (a) greater than the repeatability coefficient and (b) comparable to srT1 differences between matched participants. Future work will test the method on external validation cohorts from independent subjects with different pancreatic diseases.

Second, the automated QC only improved agreement on the internal validation dataset. As the external validation set contained fewer scans outside the limits of agreement, further work on a larger range of scanners and datasets from different sources will determine whether the automated QC approach can be generalized.

Third, the manual method used as reference may not appropriately represent "ground truth". For instance, an ROI may not adequately characterize the pancreas, particularly in cases of parenchymal heterogeneity.

Finally, the semi-automated method depends on alignment between the quantitative map and the volumetric scan from which the segmentation is derived. While manual QC was introduced to pre-filter datasets with bad alignment, some misalignment may remain, eg, due to subject motion. Future work may consider an additional registration module.[39,40]

Conclusion

Our semi-automated segmentation-based pipeline aligns well with traditional manual ROI-based reporting for pancreas MRI quantification, aided by a novel automated QC module. This tool has the potential to enhance workflow efficiency and opens up potential for a broader characterization of pancreatic diseases, paving the way for more effective patient management. Future enhancements should focus on expanding the QC module and integrating active learning for handling complex cases.

Acknowledgements

We thank the COVERSCAN team for recruitment and data collection, and all study participants. We also thank the Engineering and Physical Sciences Research Council (EPSRC) for the studentship award with reference 2280970.

Author contributions

Study design: Alexandre Triay Bagur, Zobair Arya, Daniel P. Bulte, Paul Aljabar, Michael Brady. Patient recruitment: Rajarshi Banerjee. Data collection: Rajarshi Banerjee. Data analysis: Alexandre Triay Bagur, Tom Waddell. Data interpretation: Alexandre Triay Bagur, Zobair Arya, Paul Aljabar, Michael Brady. Manuscript drafting: Alexandre Triay Bagur, Zobair Arya. All authors reviewed the article.

Supplementary material

Supplementary material is available at *BJR* online.

Funding

The COVERSCAN study was supported by the UK's National Consortium of Intelligent Medical Imaging through the Industry Strategy Challenge Fund, Innovate UK Grant 104688, and also through the European Union's Horizon 2020 research and innovation programme under grant agreement No 719445.

Conflicts of interest

A.T.B., Z.A., T.W., M.P., C.F., D.C., E.J., H.B.T.-B., M.D. R., R.B., P.A., M.B. are (or were) employees of Perspectum and hold shares and/or share options. D.P.B. declares no potential conflict of interest.

Data availability

The author will make efforts to provide data in response to reasonable requests.

References

1. Smits MM, Van Geenen EJM. The clinical significance of pancreatic steatosis. *Nat Rev Gastroenterol Hepatol*. 2011;8:169-177.
2. Takahashi M, Hori M, Ishigamori R, Mutoh M, Imai T, Nakagama H. Fatty pancreas: a possible risk factor for pancreatic cancer in animals and humans. *Cancer Sci*. 2018;109:3013-3023.
3. Tushuizen ME, Bunck MC, Pouwels PJ, et al. Pancreatic fat content and β-cell function in men with and without type 2 diabetes. *Diabetes Care*. 2007;30:2916-2921.
4. Lingvay I, Esser V, Legendre JL, et al. Noninvasive quantification of pancreatic fat in humans. *J Clin Endocrinol Metab*. 2009; 94:4070-4076.
5. Mathur A, Marine M, Lu D, et al. Nonalcoholic fatty pancreas disease. *HPB (Oxford)*. 2007;9:312-318.
6. Van Geenen EJM, Smits MM, Schreuder TCMA, Van Der Peet DL, Bloemena E, Mulder CJJ. Nonalcoholic fatty liver disease is related to nonalcoholic fatty pancreas disease. *Pancreas*. 2010; 39:1185-1190.
7. Dennis A, Kelly MD, Fernandes C, et al. Correlations between MRI biomarkers PDFF and cT1 with histopathological features of non-alcoholic steatohepatitis. *Front Endocrinol (Lausanne)*. 2020; 11:575843.
8. Ntusi NAB, Piechnik SK, Francis JM, et al. Diffuse myocardial fibrosis and inflammation in rheumatoid arthritis: insights from CMR T1 mapping. *JACC Cardiovasc Imaging*. 2015;8:526-536.
9. Liu C, Shi Y, Lan G, Xu Y, Yang F. Evaluation of pancreatic fibrosis grading by multiparametric quantitative magnetic resonance imaging. *J Magn Reson Imaging*. 2021;54:1417-1429.
10. Tirkes T, Lin C, Fogel EL, Sherman SS, Wang Q, Sandrasegaran K. T_1 mapping for diagnosis of mild chronic pancreatitis. *J Magn Reson Imaging*. 2017;45:1171-1176.
11. Wang M, Gao F, Wang X, et al. Magnetic resonance elastography and T1 mapping for early diagnosis and classification of chronic pancreatitis. *Magn Reson Imaging*. 2018;48:837-845.
12. Tirkes T, Shah ZK, Takahashi N, et al. Consortium for the Study of Chronic Pancreatitis, Diabetes, and Pancreatic Cancer. Reporting standards for chronic pancreatitis by using CT, MRI, and MR cholangiopancreatography: the consortium for the study of chronic pancreatitis, diabetes, and pancreatic cancer. *Radiology*. 2019;290:207-215.
13. Hernando D, Heijden RAVD, Reeder SB, Hernando D. A better understanding of liver T1. *Eur Radiol*. 2023;33:6841-6843.
14. Tirkes T, Yadav D, Conwell DL, et al. Consortium for the Study of Chronic Pancreatitis, Diabetes, and Pancreatic Cancer. Magnetic resonance imaging as a non-invasive method for the assessment of pancreatic fibrosis (MINIMAP): a comprehensive study design from the consortium for the study of chronic pancreatitis, diabetes, and pancreatic cancer. *Abdom Radiol (NY)*. 2019;44:2809-2821.
15. Evrimler S, Swensson JK, Are VS, Tirkes T, Vuppalanchi R, Akisik F. Quantitative assessment of disease severity of primary sclerosing cholangitis with T1 mapping and extracellular volume imaging. *Abdom Radiol (NY)*. 2021;46:2433-2443.
16. Moon JC, Messroghli DR, Kellman P, et al. Myocardial T1 mapping and extracellular volume quantification: a Society for Cardiovascular Magnetic Resonance (SCMR) and CMR Working Group of the European Society of Cardiology consensus statement. *J Cardiovasc Magn Reson*. 2013;15:92.
17. Dennis A, Cuthbertson DJ, Wootton D, et al. Multi-organ impairment and long COVID: a 1-year prospective, longitudinal cohort study. *J R Soc Med*. 2023;116:97-112.
18. CoverScan v1 510(k) Premarket Notification [https://www.accessdata.fda.gov/scripts/cdrh/cfdocs/cfpmn/pmn.cfm? ID=K212565]
19. Nadarajah C, Fananapazir G, Cui E, et al. Association of pancreatic fat content with type II diabetes mellitus. *Clin Radiol*. 2020; 75:51-56.
20. Kühn J-P, Berthold F, Mayerle J, et al. Pancreatic steatosis demonstrated at MR imaging in the general population: clinical relevance. *Radiology*. 2015;276:129-136.
21. Gilligan LA, Dillman JR, Tkach JA, Xanthakos SA, Gill JK, Trout AT. Magnetic resonance imaging T1 relaxation times for the liver, pancreas and spleen in healthy children at 1.5 and 3 tesla. *Pediatr Radiol*. 2019;49:1018-1024.
22. Ruijsink B, Puyol-Antón E, Oksuz I, et al. Fully automated, quality-controlled cardiac analysis from CMR: validation and large-scale application to characterize cardiac function. *JACC Cardiovasc Imaging*. 2020;13:684-695.
23. Kart T, Fischer M, Winzeck S, et al. Automated imaging-based abdominal organ segmentation and quality control in 20,000 participants of the UK Biobank and German National Cohort Studies. *Sci Rep*. 2022;12:18733.
24. Biasiolli L, Hann E, Lukaschuk E, et al. Automated localization and quality control of the aorta in cine CMR can significantly accelerate processing of the UK Biobank population data. *PLoS One*. 2019;14:e0212272.
25. Thrall JH, Li X, Li Q, et al. Artificial intelligence and machine learning in radiology: opportunities, challenges, pitfalls, and criteria for success. *J Am Coll Radiol*. 2018;15:504-508.
26. Dennis A, Wamil M, Alberts J, et al. COVERSCAN Study Investigators. Multiorgan impairment in low-risk individuals with post-COVID-19 syndrome: a prospective, community-based study. *BMJ Open*. 2021;11:e048391.

27. Mojtahed A, Kelly CJ, Herlihy AH, et al. Reference range of liver corrected T1 values in a population at low risk for fatty liver disease—a UK Biobank sub-study, with an appendix of interesting cases. *Abdom Radiol (NY)*. 2019;44:72-84.
28. Tunnicliffe EM, Banerjee R, Pavlides M, Neubauer S, Robson MD. A model for hepatic fibrosis: the competing effects of cell loss and iron on shortened modified Look-Locker inversion recovery T1 (shMOLLI-T1) in the liver. *J Magn Reson Imaging*. 2017; 45:450-462.
29. Bachtiar V, Kelly MD, Wilman HR, et al. Repeatability and reproducibility of multiparametric magnetic resonance imaging of the liver. *PLoS One*. 2019;14:e0214921.
30. Perspectum Ltd. *Method and System for Standardisation of a Physical Measurement*. 2023. https://www.search-for-intellectual-property.service.gov.uk/GB2315225.9
31. Owler J, Bagur AT, Marriage S, et al. *Pancreas Volumetry in UK Biobank: Comparison of Models and Inference at Scale*. Vol 12722 LNCS. Springer International Publishing; 2021.
32. Frøkjær JB, Akisik F, Farooq A, et al. Working Group for the International (IAP—APA—JPS—EPC) Consensus Guidelines for Chronic Pancreatitis. Guidelines for the diagnostic cross sectional imaging and severity scoring of chronic pancreatitis. *Pancreatology*. 2018;18:764-773.
33. Farrell JJ. Pancreatic cysts and guidelines. *Dig Dis Sci*. 2017; 62:1827-1839.
34. Harrington KA, Shukla-Dave A, Paudyal R, Do RKG. MRI of the pancreas. *J Magn Reson Imaging*. 2021;53:347-359.
35. Steinkohl E, Olesen SS, Hansen TM, Drewes AM, Frøkjær JB. T1 relaxation times and MR elastography-derived stiffness: new potential imaging biomarkers for the assessment of chronic pancreatitis. *Abdom Radiol (NY)*. 2021;46:5598-5608.
36. Triay Bagur A, Aljabar P, Ridgway GR, Brady M, Bulte DP. Pancreas MRI segmentation into head, body, and tail enables regional quantitative analysis of heterogeneous disease. *J Magn Reson Imaging*. 2022;2021.11.30.21266158.
37. Saisho Y. Pancreas volume and fat deposition in diabetes and normal physiology: consideration of the interplay between endocrine and exocrine pancreas. *Rev Diabet Stud*. 2016;13:132-147.
38. Macauley M, Percival K, Thelwall PE, Hollingsworth KG, Taylor R. Altered volume, morphology and composition of the pancreas in type 2 diabetes. *PLoS One*. 2015;10:e0126825.
39. Bagur AT, Aljabar P, Arya Z, McGonigle J, Brady SM, Bulte D. Slice-to-volume registration enables automated pancreas MRI quantification in UK Biobank. In: *Lecture Notes in Computer Science (including subseries Lecture Notes in Artificial Intelligence and Lecture Notes in Bioinformatics)*. Vol 12722 LNCS. Springer International Publishing; 2021:210-223.
40. Luo W, Bagur AT, Aljabar P, Ralli G, Brady SM. *SVRDA: A Web-based Dataset Annotation Tool for Slice-to-Volume Registration*. 2023. https://arxiv.org/abs/2311.15536

British Journal of Radiology, 2025, 98, 965–973
https://doi.org/10.1093/bjr/tqaf062
Research Article

Adverse events should be reported. Reporting forms and information can be found at www.mhra.gov.uk/yellowcard. Adverse events should also be reported to Aspire Pharma Ltd on 01730 231148.

iAluRil®

Sodium Hyaluronate | Sodium Chondroitin Sulphate | Calcium Chloride

with iAluadapter®

Effective, evidence-based[1,2] treatment for radiation-induced cystitis

Clinically proven[1,2]

Evidence-based[1,2]

Catheter-free option

The UK's number one GAG therapy[3]

Click here for Product Information

References:
1. Gacci M et al. Bladder Instillation Therapy with Hyaluronic Acid and Chondroitin Sulphate Improves Symptoms of Postradiation Cystitis: Prospective Pilot Study. Clin Genitourin Cancer 2016; Oct;14(5):444-449. 2. Giannessi C et al. Nocturia Related to Post Radiation Bladder Pain can be Improved by Hyaluronic Acid Chondroitin Sulfate (iAluRil). Euro Urol Suppl 2014; 13: e592. 3. UK IQVIA data (accessed August 2024)

iAluRil®

www.ialuril.co.uk

10102442185 v1.0 August 2024

ASPIRE® PHARMA

www.aspirepharma.co.uk